J. Chem. Sci. (2020)132:95
https://doi.org/10.1007/s12039-020-01790-5

REGULAR ARTICLE

Study of photophysical behaviour of some Sm(III) complexes with 4-oxo-4*H*-1-benzopyran-3-carboxaldehyde and other N,N′-donor π-conjugated ligands

ARCHANA CHAUHAN and RITU LANGYAN*
Department of Chemistry, Kurukshetra University, Kurukshetra, Haryana 136119, India
E-mail: ritu.langyan@gmail.com

MS received 28 January 2020; revised 10 April 2020; accepted 13 April 2020

Abstract. Trivalent lanthanide ions show interesting optical properties. Keeping this in view, five Sm(III) complexes were synthesized using 4-oxo-4*H*-1-benzopyran-3-carboxaldehyde (L) as primary ligand along with 1,10-Phenanthroline (Phen); Bipyridine (Bipy); Bathophenanthroline (Bathophen) and Neocuproine (Neo) as secondary ligands. Characterizations of prepared complexes were carried out by means of FTIR, elemental analysis, UV–vis, ESI-MS$^+$, thermal studies, PXRD, FESEM, and luminescence studies. Thermal studies confirmed the good thermal stability of complexes. Sharp peaks in X-ray diffractograms suggest their crystalline nature. The photoluminescence process in complexes has been thoroughly studied and discussed in liquid and powder state. The complexes show $^4G_{5/2} \rightarrow {}^6H_j$ transitions where j = 5/2, 7/2, and 9/2, analogous to characteristic emission peaks of Sm(III) ion at ∼ 566, 601, and 648 nm, respectively. The complexes demonstrate intense emission peaks at ∼ 601 in liquid and ∼ 648 nm in a powder state, which is responsible for bright orange and red emission, respectively. The synergistic effect of secondary ligands was responsible for longer luminescence lifetime and enhanced emission intensity in ternary complexes. Attractive photoluminescence properties of complexes could play a vital role in electroluminescent devices, bio-assays, liquid lasers, OLEDs, etc.

Keywords. Bright luminescence; Sm(III) complexes; crystalline nature; thermal studies; UV–vis; FESEM.

1. Introduction

Distinguished properties of organo-lanthanide complexes such as longer luminescence lifetime, high luminescence intensities, high quantum yield, large stoke shift, and sharp emission bands make them very efficient in the field of medical and material sciences.[1–5] Peculiar features and great potential applications of organo-lanthanides have led scientists to work tremendously in synthesizing novel lanthanide complexes with excellent thermal and photoluminescent properties. To attain high thermal stability and to avoid any material decomposition, the coordination number of Ln(III) ion in the complex should be saturated.[6] Another problem which needs to overcome is that Ln(III) ions possess weak absorption and emission due to parity forbidden transitions.[7,8] However, if appropriate organic ligands coordinate with Ln(III) ion, the absorption and emission efficiencies can be enhanced through effective energy migration from ligand to metal and this phenomenon is known as 'antenna effect'.[9]

Chromones and their derivatives are a broad class of organic heterocyclic compounds which consist of rigid bicyclic structure.[10] Extensive research on chromones and their derivatives has been done till date, and they validate great medicinal and pharmaceutical applications.[11–14] Availability of bidentate oxygen coordinating sites make chromone compounds highly reactive chelating ligands toward transition metal ions.[15–18] Due to rigid π-conjugated structure and active coordination sites, chromone compounds may act as suitable antennae ligands in enhancing luminescence intensity and thermal stability of lanthanides complexes.[19]

In this article, we report the synthesis of five Sm(III) complexes utilizing 4-oxo-4*H*-1-benzopyran-3-

*For correspondence

Electronic supplementary material: The online version of this article (https://doi.org/10.1007/s12039-020-01790-5) contains supplementary material, which is available to authorized users.

Published online: 04 August 2020

carboxaldehyde (**L**); 1, 10-Phenanthroline (**C2**); Bipyridine (**C3**); Bathophenanthroline (**C4**) and Neocuproine (**C5**). Some Ln(III) complexes with selected ligand have been reported previously.[19] However, our results differ from those reported earlier as it is also reported that different reaction media can alter chelating behaviour of chromones.[19]

Different characterization techniques like FTIR, elemental analysis, UV–vis, ESI-MS^+, thermal studies, PXRD, FESEM, and luminescence studies were employed to interpret the structure, thermal, and optical properties. Our research work is focused on improving the thermal and luminescent properties of complexes by introducing secondary ligands in the coordination sphere of complexes through the replacement of water molecules. Results obtained from photoluminescence data revealed excellent orange emission in DMSO and red emission in powder state, which is further confirmed by CIE coordinates. Prepared complexes might be practically applicable in the fields of photoelectric materials, OLEDs, biological assays, and liquid lasers.

2. Experimental

2.1 *Materials and physical measurements*

Commercially available chemicals such as $Sm(NO_3)_3.6H_2O$; 4-oxo-4*H*-1-benzopyran-3-carboxaldehyde; 1, 10-Phenanthroline; Bipyridine; Bathophenanthroline and Neocuproine were used without further purification. Distilled ethanol and double distilled water were used for reaction purpose. FTIR spectra of ligand and complexes were obtained by using the Perkin-Elmer spectrum-2 FTIR spectrophotometer between 4000 and 400 cm^{-1} range (resolution 0.5 cm^{-1}) at room temperature. Carbon, hydrogen, and nitrogen content in complexes were established using a vario MICRO CHN Elemental Analyzer. Waters Xevo G2-S QTOF spectrophotometer was used to determine Electrospray ionization mass spectra (ESI-MS^+). Thermal analysis was carried out at 10 °C/min heating rate on SII 6300 EXSTAR instrument under argon gas. The luminescence emission spectra and luminescent decay time of powder samples were recorded on Hitachi F-7000 FL spectrophotometer fitted with a xenon lamp. The luminescence profile (excitation and emission spectra) of liquid samples were carried out with RF-5301 Shimadzu spectrophotometer, respectively. The Rigaku Ultima IV instrument with CuKα radiation was used to determine powder XRD patterns. The FESEM images were obtained from the Nova nano SEM 450 instrument. T90+ UV/VIS and Perkin Elmer Lamda 900 Spectrophotometer were used to record electronic spectra of ligand and complexes in liquid and powder form, respectively.

3. Preparation of complexes

3.1 *Complex C1 [$Sm(L)_3{\cdot}2H_2O$]*

To aqueous solution of $Sm(NO_3)_3{\cdot}6H_2O$ (0.2225 g, 1 mmol), ethanol solution of Ligand **L** (0.261 g, 3 mmol) was added drop-wise, and pH value of the resultant mixture was adjusted to neutral using aqueous NaOH. After continuously stirring the resultant mixture for 3 h at 50 °C, it was left undisturbed for 2 h. The obtained precipitates were filtered and washed with water and ethanol. The residues were dried in a vacuum desiccator to get complex **C1**. The reaction was instigated by the nucleophilic attack of the solvent molecule at the second position of a ligand molecule to form an ethoxylation intermediate (4-hydroxy-2-ethoxy-2H-chromene-3-carbaldehyde).[15]

[$Sm(L)_3{\cdot}2H_2O$], ($C_{36}H_{37}O_{14}Sm$): Pale yellow powder, 68 % yield, Elemental analysis of complex **1** experimental (cal) % C, 51.39 (51.23); H, 4.67 (4.42). ESI-MS^+: [$Sm(L)_3{\cdot}2H_2O{+}H^+$] at m/z = 846.5343.

Ternary complexes **C2–C5** were synthesized in similar fashion, i.e. by mixing the solutions of $Sm(NO_3)_3{\cdot}6H_2O$, ligand **L** and secondary ligands in 1:3:1 molar stoichiometry. After maintaining a constant pH of 6.8–7, this mixture was stirred on a magnetic stirrer at 50 °C for 3 h. The obtained precipitates were filtered and washed. The synthetic route of complexes **C1–C5** is displayed in Figure 1.

3.2 *Complex C2 [$Sm(L)_3.Phen$]*

[$Sm(L)_3$.Phen], ($C_{48}H_{41}O_{12}N_2Sm$): Pale yellow powder, 72 % yield, Elemental analysis of complex **C2** experimental (cal) % C, 58.65 (58.34); H, 4.43 (4.18); N, 2.37 (2.83). ESI-MS^+: [$Sm(L)_3$.Phen+H^+] at m/z = 990.9756.

3.3 *Complex C3 [$Sm(L)_3.Bipy$]*

[$Sm(L)_3$.Bipy], ($C_{46}H_{41}O_{12}N_2Sm$): Pale yellow powder, 71 % yield, Elemental analysis of complex **C3** experimental (cal) % C, 57.79 (57.30); H, 4.15 (4.29); N, 2.94 (2.91). ESI-MS^+: [$Sm(L)_3$.Bipy+H^+] at m/z = 961.9353.

3.4 *Complex C4 [$Sm(L)_3.Bathophen$]*

[$Sm(L)_3$.Bathophen], ($C_{60}H_{49}O_{12}N_2Sm$): Pale yellow powder, 69% yield, Elemental analysis of complex **C4** experimental (cal) % C, 63.65 (63.19); H, 4.86 (4.33);

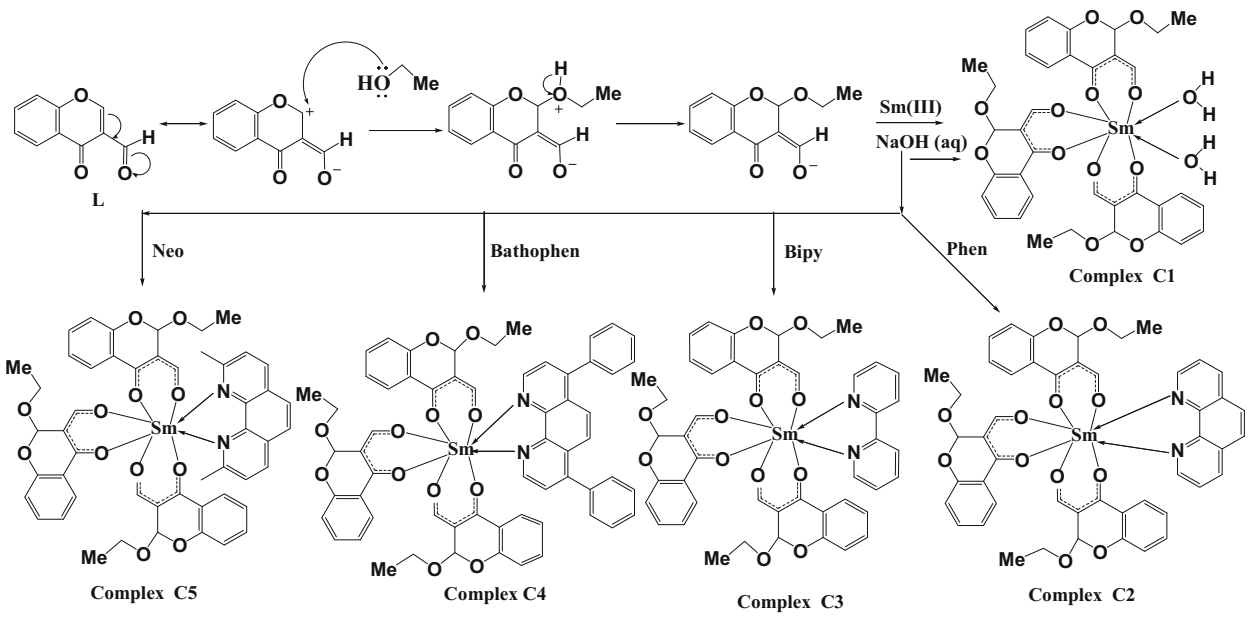

Figure 1. Synthetic route of complexes **C1–C5**.

N, 2.48 (2.46). ESI-MS$^+$: [Sm(L)$_3$.Bathophen+H$^+$] at *m/z* = 1143.0601.

3.5 *Complex C5 [Sm(L)$_3$.Neo]*

[Sm(L)$_3$.Neo], ($C_{50}H_{45}O_{12}N_2Sm$): Pale yellow powder, 72% yield, Elemental analysis of complex **C5** experimental (cal) % C, 59.65 (59.09); H, 4.49 (4.46); N, 2.98 (2.76). ESI-MS$^+$: [Sm(L)$_3$.Neo+H$^+$] at *m/z* = 1020.6292.

4. Results and Discussion

4.1 *FTIR spectra*

FTIR spectra of ligand **L** and its analogous complexes **C1–C5** were studied to investigate the changes observed on complex formation. Frequencies observed at 2867 cm^{-1}, and 1690 cm^{-1} in free ligand correspond to ν(C-H) and ν(C=O) vibration of the aldehyde group, respectively. The subsequent loss of parent aldehyde peak at 1690 cm^{-1} was due to the attack of solvent on ligand molecule and formation of a 4-hydroxy-2-ethoxy-2H-chromene-3-carbaldehyde intermediate.[15] A new peak also appeared at 2857 (C1), 2857 (C2), 2857 (C3), 2854 (C4), and 2853 (C5) corresponding to ν(C-H) stretching vibrations of ethoxy group in the complexes.[15,20]

The participation of ketone moiety in bond-formation with Sm(III) ion was established by red-shift from 1637 cm^{-1} of ν(C=O) in the complexes to 1631 (C1), 1630 (C2), 1636 (C3), 1623 (C4) and 1630 cm^{-1} (C5). The complexes display other relevant peaks at 529–545 cm^{-1} and 409–427 cm^{-1} due to ν(Sm-N) and ν(Sm-O) stretching vibrations, respectively.[9] Moreover, the complex **C1** displayed a broad spectral band from 3200 to 3500 cm^{-1}, which can be assigned to ν(O-H) vibration of coordinated water molecules.

4.2 *UV–vis spectra*

As a result of parity forbidden 4f→4f transitions, Ln(III) ions exhibit low absorption in the UV region. In other words, the spectrum of complex is masked by the absorption spectrum of ligand. UV–vis spectra of ligand **L** and complexes **C1–C5** in 10^{-5} M DMSO solution and powder state are shown in Figures 2 and 3, respectively. The spectrum of ligand **L** displayed intense absorption bands at 259 nm (38610 cm^{-1}) and 352 nm (28409 cm^{-1}) in solution and powder state, respectively. On complex formation, the absorbance maxima were shifted to 264 (37878 cm^{-1}), 265 (37735 cm^{-1}), 265 (37735 cm^{-1}), 264 (37878 cm^{-1}) and 252 nm (39682 cm^{-1}) in solution and 295 (33898 cm^{-1}), 321 (31152 cm^{-1}), 291 (34364 cm^{-1}), 316 (31645 cm^{-1}) and 268 nm (37313 cm^{-1}) in powder state for complexes **C1–C5**, respectively. The spectral bands in powder complexes were slightly blue-shifted relative to that of free ligand that shows that the singlet level of ligand L is not much affected on complex formation.[21] Due to complex formation, the metal ion induces perturbation in the electron

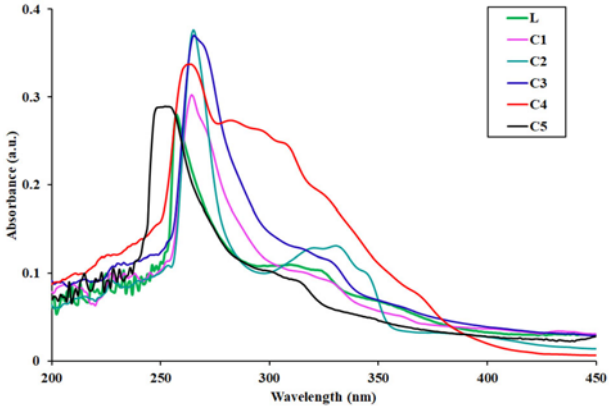

Figure 2. UV–vis spectra of ligand L and complexes **C1–C5** in 10^{-5} M DMSO.

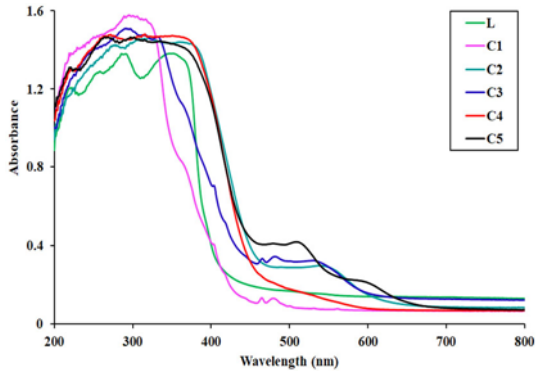

Figure 3. UV–vis spectra of ligand L and complexes **C1–C5** in a powder state.

density of ligand. As a result, the spectral bands of complexes undergo blue-shift because the electron density is shifted away from the ligand towards metal ion.[22] Since no spectral bands were noticed beyond 450 nm, the UV–vis spectra of complexes were recorded up to 450 nm in the solution phase.[23]

Furthermore, the compounds with optimal HOMO-LUMO gap are promising candidates in semi-conducting devices and photovoltaic systems.[24,25] Hence, HOMO-LUMO gap were also determined from UV–vis spectra of powder samples, using equation[26] given below:

$$\alpha \mathbf{h}\nu = \mathbf{A}(\mathbf{h}\nu - \mathbf{E}\mathrm{g})^{\mathbf{n}} \quad (1)$$

Here, α is the absorption coefficient; ν is the frequency of incident photon; h is Planck's constant; A is band tailing parameter; n is the power factor of transition mode, and E_g is optical band gap energy. The value of "n" is dependent on the type of electronic transition.[26–28] The calculated optical HOMO-LUMO gap of complexes **C1–C5** from Tauc's plot was found to be 3.12, 2.89, 3.06, 2.87, and 2.89 eV. The complexes have the capability to be used as semiconducting materials in photovoltaic systems, since their optical energies are larger than other commonly used semiconductors.[29,30]

4.3 *PXRD and FESEM*

The powder X-ray diffraction analysis is a widely used technique for the determination of crystallinity in organic and inorganic compounds. Since the crystalline nature of luminescent materials plays an important role in photonic devices, the powder XRD data of prepared complexes were recorded to get an idea about their crystalline behaviour.[31–33] The diffractograms of complexes **C1–C5** exhibited well-defined sharp peaks between 10 and 50° at 2θ angle as shown in Figure 4. This shows crystalline nature of complexes and the average size of crystallites can be theoretically calculated from Debye-Scherrer's formula[34] as follows:

$$D = \frac{0.941\lambda}{\beta \cos\theta} \quad (2)$$

where, 0.941 is a constant known as shape factor; λ is X-ray wavelength; β is full-width at half-maximum (FWHM) of the intense peak; D is average crystallite size and, θ is diffraction angle. The average experimental size of crystallites was 42.9 (**C1**), 45.1 (**C2**), 47.6 (**C3**), 47.6 (**C4**) and, 50.4 nm (**C5**).

FESEM helped in determining the microstructure and surface morphology of complexes. All the parameters involved are represented on the image itself. The micrograph of complex **C1** represented homogenous morphology having regular rod-shaped particles.[35] Micrograph of complex **C2** demonstrated

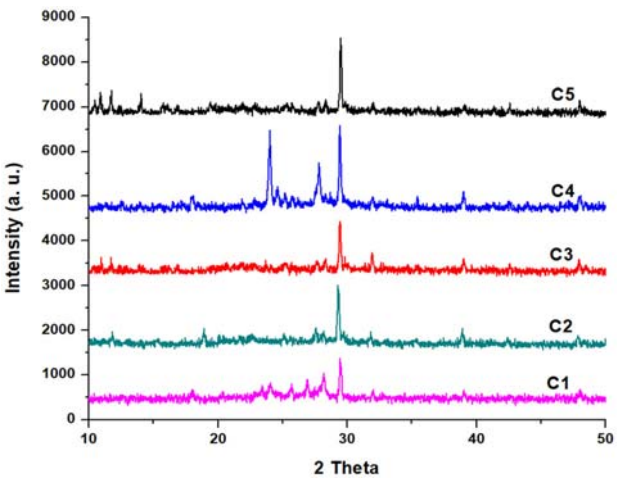

Figure 4. Powder XRD of complexes **C1–C5**.

snow-bush morphology, and the particles size was 5 μm.[31] Metal complexes having uniform morphology, narrow particle size and crystalline nature play a vital role as luminescent materials in photonic devices and these conditions are satisfied by the synthesized complexes.[33]

4.4 *Luminescence properties*

4.4.1 *PL excitation*: Excitation spectra (Figure 5) of complexes **C1–C5** were obtained in DMSO solution (10^{-5} M) at 601 nm emission wavelength at RT. The spectra are broad bands with maximum absorbance at 378, 390, 383, 394, and 386 nm for complexes **C1–C5**, respectively, which corresponds to the intra-ligand excitation transition of organic ligands.

4.4.2 *PL emission*: Photoluminescence spectra of complexes were recorded at room temperature in 10^{-5} M DMSO solution and powder state on excitation with 370 nm wavelength. On absorption of UV light, the complexes emit bright luminescence in liquid and powder states, and their emission spectra are given in Figures 6 and 7, respectively. The complexes show characteristic Sm(III) ion spectral bands which arise from f–f transitions $^4G_{5/2}\rightarrow{}^6H_{5/2}$ (∼ 566 nm), $^4G_{5/2}\rightarrow{}^6H_{7/2}$ (601 nm) and $^4G_{5/2}\rightarrow{}^6H_{9/2}$ (648 nm) have $\Delta J = 0$, 1 and 2 respectively, where J is total angular momentum.[36,37] In DMSO solution spectral bands at ∼ 566 nm is the magnetic-dipole transition, 601 nm is mixed magnetic-electric dipole transition, and 648 nm is electric dipole transition while in a powder state, the $^4G_{5/2}\rightarrow{}^6H_{7/2}$ is magnetic-dipole transition and hypersensitive $^4G_{5/2}\rightarrow{}^6H_{9/2}$ is electric dipole transition.[38] The complexes exhibit orange emission in DMSO solution due to most intense $^4G_{5/2}\rightarrow{}^6H_{7/2}$ transition at ∼ 601 nm. The stark splitting observed in $^4G_{5/2}\rightarrow{}^6H_{7/2}$ transition corresponds to asymmetry in the complexes.[39] The intensities of luminescence bands are sensitive towards the nature of ligand environment; thus, dissimilar emission spectra of complexes were observed in solution and powder state.[40,41] The electric dipole transition at ∼ 648 nm was most dominant, and this enhanced transition was responsible for intense red emission in complexes. The strong and narrow emission of electric dipole transition supports lower asymmetric local environment around Sm(III) ion.[42,43] If a metal centre is situated in a highly asymmetric environment, the luminescence intensity is greatly enhanced. The presence of high vibronic coupling C-H or O-H oscillators of solvent molecules quenches the excited state of Sm(III) ion in solution.[37] Hence, the relative emission intensity of complexes in solution was lower than in powder state. Also, high vibrational

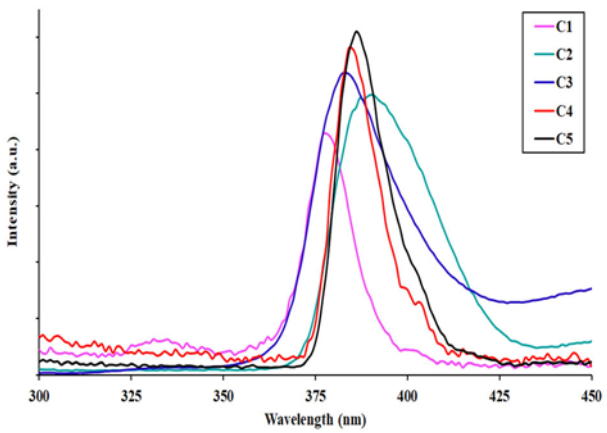

Figure 5. Excitation spectra of complexes **C1–C5** (in 10^{-5} M DMSO) at RT, λ_{em} is 600 nm.

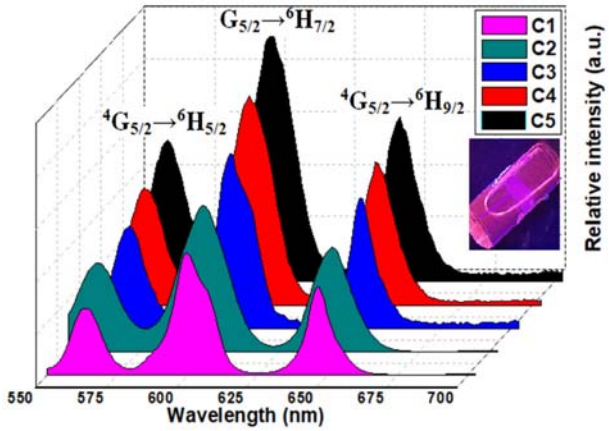

Figure 6. Emission spectra of complexes **C1–C5** at RT in 10^{-5} M DMSO, λ_{ex} is 370 nm.

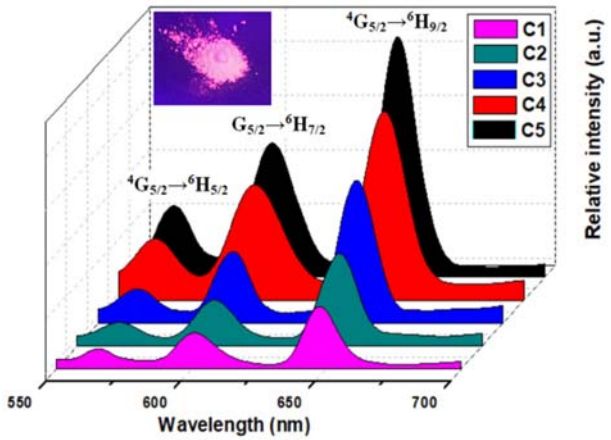

Figure 7. Emission spectra of powder complexes **C1–C5** at RT, λ_{ex} is 370 nm.

energy O-H bonds of coordinated water molecules quench the luminescence efficiency of binary complex **C1**.

Introduction of secondary ligands increases the π-conjugation in ternary complexes and lower the non-radiative loss of energy due to O-H vibrations from water molecules.[32] As a consequence of extended π-conjugation, the ligand energy levels are lowered, and energy migrates from ligand triplet state to resonant level of central metal ion very efficiently.[43] Hence, the emission intensity of ternary complexes **C2–C5** was comparatively higher than that of binary complex C1.[7,33] Ternary complex **C5** (consisting of **neo**) has the highest emission intensity, this may be attributed to the presence of electron-donating methyl moieties which tend to increase electron density on Sm(III) ion.[32] Complex **C4** also has electron-donating phenyl groups on bathophen, but these groups create steric hindrance which results in the reduction of emission intensity of **C4** as compared to that of **C5**.[44]

4.4.3 *Quantum yield, color chromaticity and decay time*: To explore the effect of secondary ligands on emission intensity of Sm(III) ion, luminescence quantum yield of complexes **C1–C5** (ϕ_s) was calculated in DMSO solution with the help of equation (3), against standard quinine bisulphate in 0.5 mol H_2SO_4 (ϕ_{st} = 0.546 and $\eta = 1.333$)[45]:

$$\phi_s = \frac{\phi_{st}\, I_s\, A_{st}\, n_s^2}{I_{st}\, A_s\, n_{st}^2} \quad (3)$$

Where, s and st imply sample and reference, respectively; I is integrated luminescence intensity; A is the absorbance at the excitation wavelength and, η is the refractive index of solvent. The refractive index is considered equivalent to that of the pure solvent. The obtained values of luminescence quantum yield for complexes **C1–C5** were equivalent to those attained from diketones and carboxylic acids.[46–49] Hence, the selected ligands act as efficient sensitizers.

Color coordinates (x, y) of complexes in DMSO solution and powder state are represented in Figure 8, and the values of coordinates and quantum yield are given in Table 1. The relative intensity of orange (in DMSO) and red (powder state) emission increases as we move from binary to ternary complexes.

The luminescence lifetimes of powder complexes **C1–C5** were obtained on F-7000 FL spectrophotometer by monitoring dominant emission transition ($^4G_{5/2} \rightarrow {}^6H_{9/2}$) at 648 nm. The luminescence decay times were derived from the following equation:

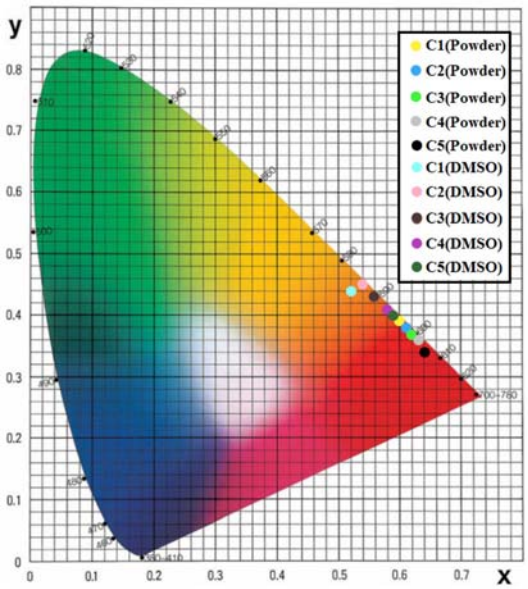

Figure 8. CIE color coordinate diagram of complexes **C1–C5** in DMSO and powder state.

$$I = I_0 \exp\left(-t/\tau\right) \quad (4)$$

where, I signifies emission intensity at time 0; I_0 denotes emission intensity at a time, and τ denotes luminescence decay time.[50] The decay curves (Figure 9) exhibited mono-exponential behaviour. The lower lifetime value for **C1** may be attributed to non-radiative decay *via* the vibronic coupling of coordinated water molecules.[51] The ternary complexes **C2–C5** exhibited greater lifetime values that revealed the role of secondary ligands in suppressing non-radiative deactivation process and enhancing luminescence intensities.[32] All the spectral data, color coordinates, quantum yield, and decay time of complexes **C1–C5** (in solution and powder state) are summarized in Table 1.

4.4.4 *Energy transfer*: Binary complex $Gd(L)_3{\cdot}2H_2O$ was prepared using the same procedure as for complex **C1**, and its phosphorescence spectrum was recorded at room temperature for determining the triplet energy level of organic ligand **L**. Gd(III) does not emit in the visible region since its energy levels are placed above 32000 cm^{-1}, this value is considerably higher than the excited levels of ligands.[52] So, it is impossible for Gd(III) ion to accept energy from organic ligands. As no emission from Gd(III) ion is observed, so phosphorescence ($T_1 \rightarrow S_0$) spectrum is obtained purely from ligand **L**.[53] The singlet and triplet energy levels of secondary ligands (phen, bipy and bathophen) except neo have been obtained from the literature.[23] The proposed energy transfer

Table 1. Photoluminescence data, CIE coordinates, quantum yield and decay time of complexes **C1–C5.**

Complexes	Medium	Emission λ_{max} (nm)			x, y coordinates	Quantum yield (%)	Decay time τ (ms)
		$^4G_{5/2}\rightarrow{}^6H_{5/2}$	$^4G_{5/2}\rightarrow{}^6H_{7/2}$	$^4G_{5/2}\rightarrow{}^6H_{9/2}$			
C1	Solid	566	601	648	0.60, 0.39	–	0.412
	DMSO	564	600	647	0.52, 0.44	0.9	–
C2	Solid	566	601	647	0.61, 0.38	–	0.454
	DMSO	560	598	644	0.54, 0.45	1.2	–
C3	Solid	565	601	646	0.62, 0.37	–	0.466
	DMSO	564	600	647	0.56, 0.43	1.2	–
C4	Solid	563	600	648	0.63, 0.36	–	0.501
	DMSO	561	599	644	0.58, 0.41	1.6	–
C5	Solid	563	599	646	0.64, 0.34	–	0.507
	DMSO	562	599	645	0.59, 0.40	1.8	–

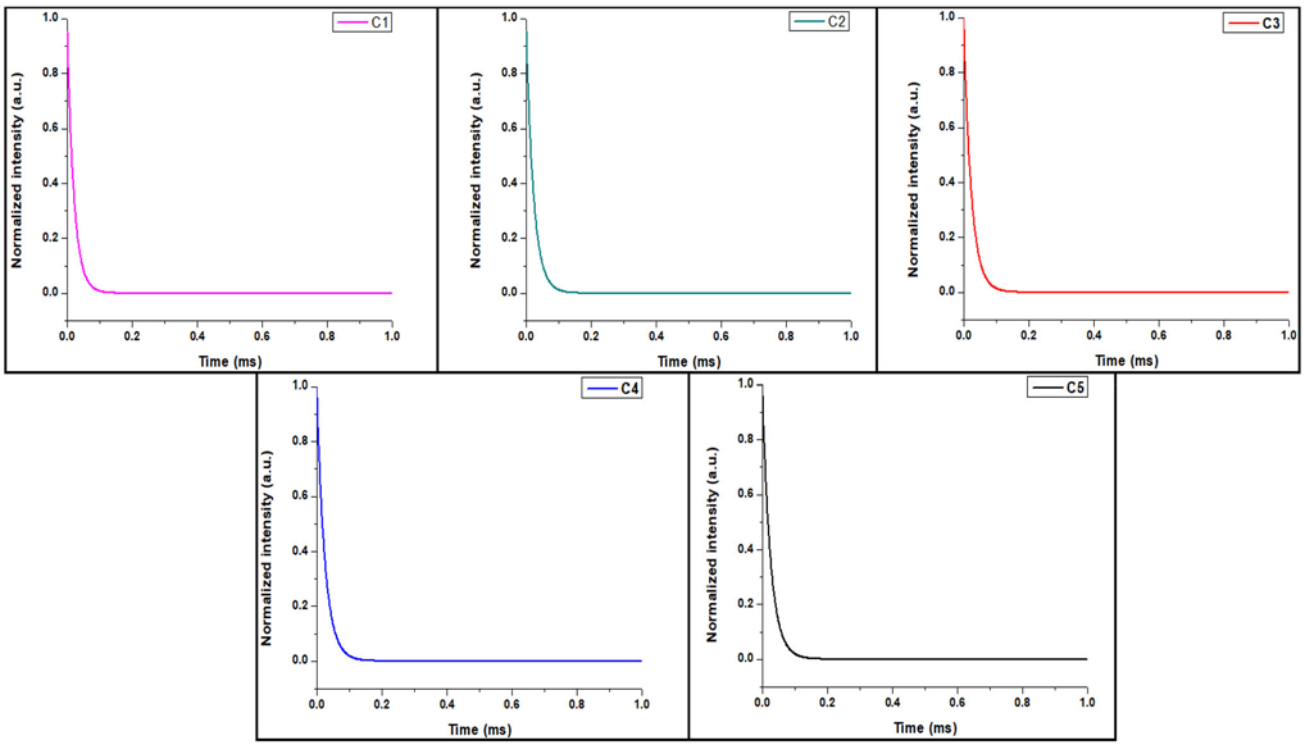

Figure 9. Luminescence decay curves of powder complexes **C1–C5** at room temperature.

mechanism is depicted in Figure 10. The energy transfer mechanism in complex **C5** can be assumed to be similar as in complexes **C2–C4** on the basis of results obtained from luminescence intensity, quantum yield, and lifetime values. The singlet excited energy level (S_1) of ligand **L** was found to be 25000 cm^{-1}, which is estimated from edge wavelength of its UV–vis spectrum.[44] Triplet energy level (T_1 = 21881 cm^{-1}) was determined from lower emission edge wavelength of phosphorescence spectrum. As observed from photoluminescence data, the resonant level ($^4G_{5/2}$) of Sm(III) was situated at ∼ 17730 cm^{-1} (∼ 566 nm). The effectiveness of intramolecular energy transfer from ligand to lanthanide ion depends on the energy gap between triplet level of ligand **L** and resonant level of lanthanide ion.[54] The energy gap ΔE between T_1 of ligand **L** and $^4G_{5/2}$ level of Sm(III) was ∼ 4151 cm^{-1}, which satisfies the condition for effective intramolecular energy migration between ligand

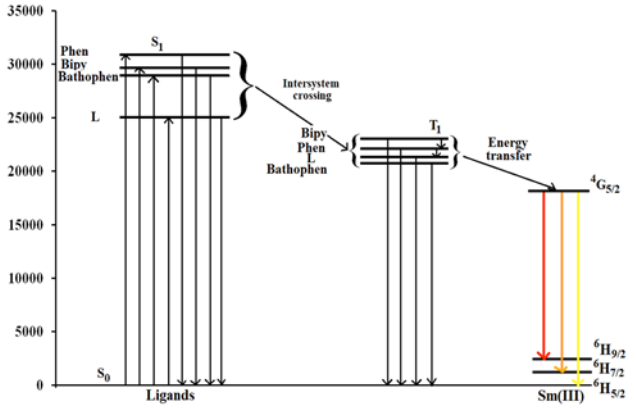

Figure 10. The proposed energy transfer mechanism in complex **C1–C4.**

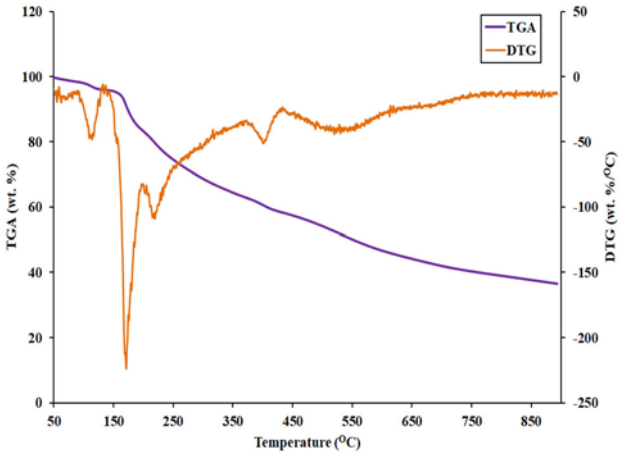

Figure 11. TGA/DTG curve of complex C1.

L and Sm(III) ion.[55] All the results indicate that the selected ligand **L** is an efficient sensitizer for Sm(III) ion. The corresponding energies of ligands L, phen, bipy and bathophen are tabulated in Table 2.

4.5 *Thermal analysis*

Thermal degradation curves of complexes were obtained under the argon atmosphere to check the stability and pure decomposition of complexes in inert environment.[56,57] Complexes (**C2–C5**) exhibited similar thermal decomposition patterns, so the TGA/DTG curve of complex **C2** is taken as a representative example for all ternary complexes (Figure 12). As shown in Figure 11, the complex **C1** exhibited initial mass loss of 4.14% (found 4.27%) up to 125 °C, ascribed to loss of coordinated water molecules. Above 160 °C, the continuous loss was ascribed to the decomposition of organic ligand moiety. The ternary complexes exhibited no loss up to 180 °C, confirming the absence of coordinated water molecules. Above 700 °C, stable metal oxides were obtained. The weight of residue is higher compared to that of the calculated

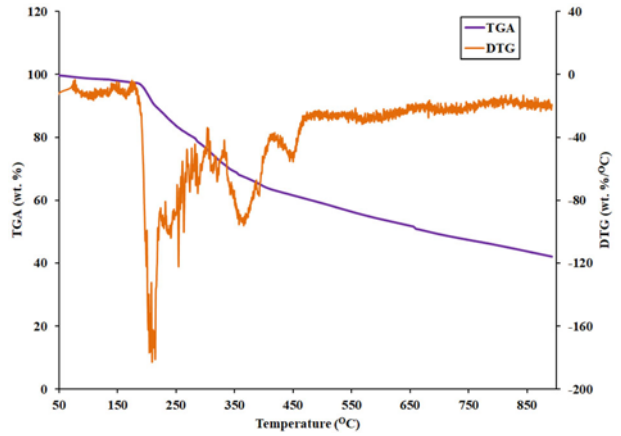

Figure 12. TGA/DTG curve of complex C2.

one, and it may be assigned to the formation of ashes of organic ligand due to incomplete decomposition, thus revealing higher thermal stability.[58,59] The complexes **C2–C5** possess higher thermal stability up to 180 °C. Hence, they can be employed as luminescent materials in light-emitting devices.[60]

Table 2. The energies of ligand L, phen, bipy and bathophen.

Ligands	Excited level	Energy of excitation level (cm^{-1})	ΔE ($S_1 - T_1$) (cm^{-1})	ΔE ($T_1 - {}^4G_{5/2}$) (cm^{-1})
Phen	Singlet (S_1)	31000	8900	4370
	Triplet (T_1)	22100		
Bipy	Singlet (S_1)	29900	7000	5170
	Triplet (T_1)	22900		
Bathophen	Singlet (S_1)	29000	8000	3270
	Triplet (T_1)	21000		
L	Singlet (S_1)	25000	3119	4151
	Triplet (T_1)	21881		

5. Conclusions

The reaction of Sm(III) salt with 4-oxo-4*H*-1-benzopyran-3-carboxaldehyde (**L**) and other ancillary ligands such as 1,10-Phenanthroline (Phen); Bipyridine (Bipy); Bathophenanthroline (Bathophen) and Neocuproine (Neo) resulted in the formation of orange-red luminescent complexes. Characterization of synthesized complexes was done by means of FTIR, elemental analysis, UV–vis, ESI-MS^+, thermal studies, PXRD, FESEM, and luminescence studies. The ternary complexes having N,N'-donor π-conjugated ligands exhibited higher thermal stability up to 180 °C. The crystalline nature of complexes was confirmed by PXRD. The brilliant luminescence of complexes is attributed to asymmetrical structures. In the case of binary complex, the vibronic coupling of high energy O-H oscillators of water molecules is responsible for non-radiative dissipation of energy, resulting in quenching of luminescence and lower quantum yield. Higher quantum yield and longer luminescence lifetime of ternary complexes indicate effective photosensitization of Sm(III) ion by the ligands. The selected ligands act as efficient sensitizers as they transfer energy to the lowest emitting level of Sm(III) ion via antenna effect. The simple synthesis, excellent luminescence, high thermal stability, and color tunability facilitate the synthesized complexes to become useful agents in material science.

Supplementary Information (SI)

The ESI-MS^+ spectra of complexes **C1–C5** are given in Figures S1–S5. The results of elemental analysis of complexes **C1–C5** are shown in Figure S6. The FTIR spectra of ligand **L** and its corresponding complexes **C1–C5** have been shown in Figures S7–S12. The Tauc's plots of complexes **C1–C5** are represented in Figure S13. The PXRD data, d-spacing, and intensity of most intense peaks observed in complexes **C1–C5** are tabulated in Table S1. The FESEM image of complex **C1** is shown in Figures S14, whereas the FESEM image of complex C2 is displayed in Figure S15. The Phosphorescence spectrum of powder complex $Gd(L)_3{\cdot}2H_2O$ measured at room temperature is presented in Figures S16. Supplementary information is available at www.ias.ac.in/chemsci.

Acknowledgements

We are thankful to the University Grants Commission (UGC), India for providing financial support to Archana Chauhan in the form of SRF (Senior Research Fellowship) with Award No: 19/06/2016 (i) EU-V. Authors also acknowledge MRC MNIT, Jaipur for availing ESI-MS^+, FTIR, UV–vis and FESEM characterization facilities.

Conflict of interest The authors declare no conflict of interest.

References

1. Jastrzab R, Nowak M, Skrobanska M, Tolinska A, Zabiszak M, Gabryel M, Marciniak L and Kaczmarek M T 2019 DNA as a target for lanthanide(III) complexes influence *Coord. Chem. Rev*. **382** 145
2. Wu J, Liu H, Yang Y, Wang H and Yang M 2018 A β-diketone-europium(III) complex-based time gated luminescence probe for selective visualization of peroxynitrite in living cells *Opt. Mater*. **77** 170
3. Zhao S, Wang G, Poelman D and Voort P V D 2018 Luminescent lanthanide MOFs: a unique platform for chemical sensing *Materials* **11** 572
4. Dandekar M P, Itankar S B, Kondawar S B, Nandanwar D V and Koinkar P 2018 Photoluminescent electrospun europium complex $Eu(TTA)_3$phen embedded polymer blends nanofibres *Opt. Mater*. **85** 483
5. Zheng Y, Fu L, Zhou Y, Yu J, Yu Y, Wang S and Zhang H 2002 Electroluminescence based on a β-diketonate ternary samarium complex *J. Mater. Chem*. **12** 919
6. Debroye E, Ceulemans M, Elst L V, Laurent S, Muller R N and Parac-Vogt T N 2014 Controlled synthesis of a novel heteropolymetallic complex with selectively incorporated lanthanide(III) ions *Inorg. Chem*. **53** 1257
7. Misra S N and Sommerer S O 1991 Absorption spectra of lanthanide complexes in solution *Appl. Spectrosc. Rev*. **26** 151
8. Leif R C, Vallarino L M, Becker M C and Yang S 2006 Increasing the luminescence of lanthanide complexes *Cytometry Part A*: **69A** 767
9. Nandal P, Kumar R, Khatkar A, Khatkar S P and Taxak V B 2016 Synthesis, characterization, enhanced photoluminescence, antimicrobial and antioxidant activities of novel Sm(III) complexes containing 1-(2-hydroxy-4,6-dimethoxyphenyl)ethanone and nitrogen containing ancillary ligands *J. Mater. Sci.: Mater. Electron*. **27** 878
10. Sosnovskikh V 2003 Synthesis and reactions of halogen-containing chromones *Russ Chem Rev*. **72** 489
11. Khan K M, Ambreen N, Mughal U R, Jalil S, Perveen S and Choudhary M I 2010 3-Formylchromones: potential antiinflammatory agents *Eur. J. Med. Chem*. **45** 4058
12. Ishar M P S, Singh G, Singh S, Sreenivasan K K and Singh G 2006 Design, synthesis, and evaluation of novel 6-chloro-/fluorochromone derivatives as potential topoisomerase inhibitor anticancer agents *Bioorg. Med. Chem. Lett*. **16** 1366
13. Pick A, Muller H, Mayer R, Haenisch B, Pajeva I K, Weigt M, Bonisch H, Muller C E and Wiese M 2011 Structure-activity relationships of flavonoids as inhibitors of breast cancer resistance protein (BCRP) *Bioorg. Med. Chem*. **19** 2090
14. Nowakowska Z 2007 A review of anti-infective and anti-inflammatory chalcones *Eur. J. Med. Chem*. **42** 125
15. Yousuf I, Arjmand F, Tabassum S, Toupet L, Khan R A and Siddiqui M A 2015 Mechanistic insights into a novel chromone-appended Cu(II) anticancer drug entity: *in vitro* binding profile with DNA/RNA

substrates and cytotoxic activity against MCF-4 and HepG2 cancer cells *Dalton Trans*. **44** 10330
16. Shebl M, Adly O M I, Taha A and Elabd N N 2017 Structural variety in copper(II) complexes of 3-formylchromone: synthesis, spectral, thermal, molecular modeling and biological studies *J. Mol. Struct.* **1147** 438
17. Adly O M, El-Shafiy H F 2019 New metal complexes derived from *S*-benzyldithiocarbazate (SBDTC) and chromone-3-carboxaldehyde: synthesis, characterization, antimicrobial, antitumor activity and DFT calculations *J. Coord. Chem*. **72** 218
18. Philip J E, Shahid M, Kurup M R P and Velayudhan M P 2017 Metal based biologically active compounds: design, synthesis, DNA binding and antidiabetic activity of 6-methyl-3-formyl chromone derived hydrazones and their metal (II) complexes *J. Photochem. Photobiol. B* **175** 178
19. Castellani C B, Carugo O, Tomba C and Gamba A I 1988 Fluorescent lanthanide complexes. 1. Reaction between Tb^{3+} and 4-Oxo-*4H*-1-benzopyran-3-carboxaldehyde in alcoholic medium *Inorg. Chem*. **27** 3965
20. Kalanithi M, Kodimunthiri D, Rajarajan M and Tharmaraj P 2011 Synthesis, characterization and biological activity of some new VO(IV), Co(II), Ni(II), Cu(II) and Zn(II) complexes of chromone based NNO Schiff base derived from 2-aminothiazole *Spectrochim. Acta Part A* **82** 290
21. Bala M, Kumar S, Chahar S, Taxak V B, Boora P and Khatkar S P 2020 Synthesis, NMR, and optical features of intense green color terbium(III) complexes *Optik*. **202** 163636
22. Song X Q, Zheng Q F, Wang L and Liu W S 2011 Synthesis and luminescence properties of lanthanide complexes with a new tripodal ligand featuring *N*-thenylsalicylamide arms *Luminescence*. **27** 459
23. Devi R, Dalal M, Bala M, Khatkar S P, Taxak V B and Boora P 2016 Synthesis, photoluminescence features with intramolecular energy transfer and Judd-Ofelt analysis of highly efficient europium(III) complexes. *J. Mater. Sci.: Mater. Electron*. **27** 878
24. Yan Z S, Gong Y and Lin H J 2017 Metal complexes based on 2-(5-(3,5-dibromophenyl)-2*H*-1,2,4-triazol-3-yl) pyridine and their composites with $CH_3NH_3PbI_3$: structures, band gaps and enhanced optoelectronic properties *Eur. J. Inorg. Chem*. **9** 1256
25. Za'aba N K, Sarjidan M A Mohd, Majid W H Abd, Kusrini E and Saleh M I 2014 Junction properties and conduction mechanism of new terbium complexes with triethylene glycol ligand for potential application in organic electronic device *J. Rare Earths* **32** 633
26. Tauc J, Grigorovici R and Vancu A1966 Optical properties and electronic structure of amorphous germanium *Phys. Status Solidi*. **5** 627
27. Ren S, Jiang W, Wang Q, Li Z, Qiao Y and Che G 2019 Synthesis, structures and properties of six lanthanide complexes based on a 2-(2-carboxyphenyl)imidazo(4,5-f)-(1,10)phenanthroline ligand *RSC Adv*. **9** 3102
28. Zhang D, Chen W and Wang Y 2017 A novel samarium complex with interesting photoluminescence and semiconductive properties *Bull. Chem. Soc. Ethiop*. **31** 435
29. Tillinski R, Rumpf C, Nather C, Durichen P, Jeb I, Schunk S A and Bensch W 1998 Synthesis, crystal structures, and optical properties of new quaternary metal chacogenides of Group 5: Cs_2AgVS_4, K_2AgVSe_4, Rb_2AgVSe_4, $Rb_2AgNbSe_4$, and $Cs_2AgNbSe_4$ *Z. Anorg. Allg. Chem*. **624** 1285
30. Zhou Y, He Q, Yang Y, Zhong H, He C, Sang G, Liu W, Yang C, Bai F and Li Y 2008 Binapthyl-containing green- and red-emitting molecules for solution-processable organic light-emitting diodes *Adv. Funct. Mater*. **18** 3299
31. Sengar M and Narula A K 2019 Luminescence sensitization of Eu(III) complexes with aromatic Schiff base and N,N'-donor heterocyclic ligands: synthesis, luminescent properties and energy transfer *J. Fluoresc*. **29** 111
32. Bala M, Kumar S, Boora P, Taxak V B, Khatkar A and Khatkar S P 2014 Enhanced optoelectronics properties of europium(III) complexes with β-diketone and nitrogen heterocyclic ligands *J. Mater Sci: Mater Electron.* **25** 2850
33. Dhania S L, Chauhan A and Langyan R 2020 Synthesis, Characterization and photoluminescent properties of Eu(III) complexes with 5-hydroxy-2-hydroxymethyl-4H-4-pyranone and *N,N'*-donor heterocyclic coligands. Accepted manuscript: *Rare Met*. https://doi.org/10.1007/s12598-020-01387-4
34. Ain Q, Pandey S K, Pandey O P and Sengupta S K 2016 Synthesis, structural characterization and biological studies of neodymium(III) and samarium(III) complexes with mercaptotriazole Schiff bases *Appl. Organometal. Chem*. **30** 102
35. Yao J, Tjandra W, Chen Y Z, Tam K C, Ma J and Soh B 2003 Hydoxyapatite nanostructure material derived using cationic surfactant as a template *J. Mater. Chem*. **13** 3053
36. Ahmed Z, Dar W A and Iftikhar K 2012 Syntheses and spectroscopic studies of volatile low symmetry lanthanide(III) complexes with monodentate 1H-indazole and fluorinated β-diketone *J. Coord. Chem*. **65** 3932
37. Hasan N and Iftikhar K 2019 Syntheses, crystal structure and photophysical properties of $[Sm(dbm)_3(impy)]$ and $[Tb(dbm)_3(impy)]$ and their hybrid films. *New J. Chem*. **43** 4391
38. Dar W A, Ganaie A B and Iftikhar K 2018 Synthesis and photoluminescence study of two new complexes $[Sm(hfaa)_3(impy)_2]$ and $[Eu(hfaa)_3(impy)_2]$ and their PMMA based hybrid films *J. Lumin*. **202** 438
39. Iftikhar K and Dar W A 2016 Phase controlled color tuning of the samarium and europium complexes and excellent photostability of their PVA encapsulated materials. structural elucidation, photophysical parameters and energy transfer mechanism in Eu^{3+} complex by Sparkle/PM3 calculations *Dalton Trans*. **44** 8956
40. Lis S 2002 Luminescence spectroscopy of lanthanide(III) ions in solution *J. Alloys Compd*. **341** 45
41. Bunzli J C G 1989 In *Lanthanide probes in life, chemical and earth sciences: theory and practice* (Elsevier Science: Amsterdam) p 432
42. Teotonio E E S, Felinto M C F C, Brito H F, Malta O L, Trindade A C, Najjar R and Strek W 2004 Synthesis,

crystalline structure and photoluminescence investigations of the new trivalent rare earth complexes (Sm^{3+}, Eu^{3+} and Tb^{3+}) containing 2-thiophenecarbxylate as sensitizer *Inorg. Chim. Acta* **357** 451
43. Ahmed Z, Dar W A and Iftikhar K 2012 Synthesis and luminescence study of a highly volatile Sm(III) complex. *Inorg. Chim. Acta* **392** 446
44. Bala M, Kumar S, Taxak V B, Boora P and Khatkar S P 2015 Synthesis, photoluminescent features and intramolecular transfer mechanism of europium (III) complexes with fluorinate β-diketone ligand and auxiliary ligands *J. Fluor. Chem*. **178** 6
45. Demas J N and Crosby G A 1971 The measurement of photoluminescence quantum yields. A review *J. Phys. Chem*. **75** 991
46. Klink S I, Hebbink G A, Grave L, Alink P G and Veggel F C 2002 Synergistic complexation of Eu^{3+} by a polydentate ligand and a bidentate antenna to obtain ternary complexes with high luminescence quantum yields *J. Phys. Chem. A*. **106** 3681
47. Silva F R G, Malta O L, Reinhard C, Gudel H, Piguet C, Moser J E and Bunzli J C 2002 Visible and near-infrared luminescence of lanthanide-containing dimetallic triple-stranded helicates: energy transfer mechanisms in the Sm^{III} and Yb^{III} molecular edifices *J. Phys. Chem. A*. **106** 1670
48. Li H, Wu J, Huang W, Zhou Y, Li H, Zheng Y and Zuo J 2009 Synthesis and photoluminescent properties of five homodinuclear lanthanide (Ln^{3+} = Eu^{3+}, Sm^{3+}, Er^{3+}, Yb^{3+}, Pr^{3+}) complexes *J. Photochem. Photobiol. A: Chem.* **208** 110
49. Castellani C B, Carugo O 1989 Studies on fluorescent lanthanide complexes. new complexes of lanthanide(III) with coumarinic-3-carboxylic acid *Inorg. Chim. Acta*. **159** 175
50. Sabbatini N, Guardigli M and Lehn J M 1993 Luminescent lanthanide complexes as photochemical supramolecular devices *Coord. chem. Rev*. **123** 201
51. Raj D B A, Biju S and Reddy M L P 2008 One-, two-, and three-dimensional arrays of Eu^{3+}-4,4,5,5-pentafluoro-1-(napthalen-2-yl)pentane-1,3-dione complexes: synthesis, crystal structure and photophysical properties *Inorg. Chem*. **47** 8091
52. Zhang Q, Yang X, Deng R, Zhou L, Yang Y and Li Y 2019 Synthesis and near infrared luminescent properties of a series of lanthanide complexes with POSS modified ligands *Molecules* **24** 1253
53. Brito H F, Malta O L, Felinto M C, Teotonio E E, Menezes J F, Silva C F, Tomiyama C S and Carvalho C A 2002 Luminescence investigation of the Sm(III)- β-diketonates with sulfoxides, phosphine oxides and amide ligands *J. Alloys Compd*. **344** 293
54. Dexter D L 1953 A theory of sensitized luminescence in solids *J Chem. Phys*. **21** 836
55. Latva M, Takalo H, Mukkala V, Matachescu C, Rodriguez-Ubis J C, Kankare J 1997 Correlation between the lowest triplet state level of the ligand and lanthanide(III) luminescence quantum yield *J. Lumin*. **75** 149
56. Yang C, Luo J, Ma J, Lu M, Liang L and Tong B 2011 Synthesis and photoluminescent properties of four novel trinuclear europium complexes based on two tris-β-diketones ligands *Dyes Pigm*. **92** 696
57. Liu J, Ren N, Zhang J and Zhang C 2013 Preparation, thermodynamic property and antimicrobial activity of some rare-earth (III) complexes with 3-bromo-5-iodobenzoic acid and 1,10-phenanthroline. *Thermochim Acta*. **570** 51
58. Taha Z A, Ajlouni A M and Momani W A 2012 Structural, luminescence and biological studies of trivalent lanthanide complexes with N,N'-bis(2-hydroxynapthylmethylidene)-1, 3-propanediamine Schiff base ligand *J. Lumin*. **132** 2832
59. Lin M, Wang X, Tang Q, An Q, Zeng H and Ling Q 2014 Study of yellow luminescence of binary terbium complexes based on 3,3',4,4'-biphthalic anhydride *Appl. Opt*. **53** 447
60. Poonam, Kumar R, Boora P, Khatkar A, Khatkar S P and Taxak V B 2016 Synthesis, photoluminescence and biological properties of terbium(III) complexes with hydroxyketone and nitrogen containing heterocyclic ligands *Spectrochimica Acta Part A* **152** 304